

Submitted to ApJ Letters

**Extreme Enhancements of r-process Elements in the Cool Metal-Poor
Main-Sequence Star SDSS J2357–0052**

Wako Aoki^{1,2}*National Astronomical Observatory, Mitaka, Tokyo, 181-8588 Japan*

aoki.wako@nao.ac.jp

Timothy C. Beers³*Department of Physics and Astronomy and JINA: Joint Institute for Nuclear Astrophysics,
Michigan State University, East Lansing, MI 48824-1116*

beers@pa.msu.edu

Satoshi Honda⁴*Kwasan Observatory, Kyoto University, Ohmine-cho Kita Kazan, Yamashina-ku, Kyoto, 607-847,
Japan; honda@kwasan.kyoto-u.ac.jp*

and

Daniela Carollo^{5,6}*Research School of Astronomy & Astrophysics, Australian National University
& Mount Stromlo Observatory, Cotter Road, Weston, ACT, 2611, Australia*

carollo@mso.anu.edu.au

ABSTRACT

We report the discovery of a cool metal-poor, main-sequence star exhibiting large excesses of r-process elements. This star is one of two newly discovered cool subdwarfs (effective temperatures of 5000 K) with extremely low metallicity ($[\text{Fe}/\text{H}] < -3$) identified from follow-up high-resolution spectroscopy of metal-poor candidates from the Sloan Digital Sky Survey. SDSS J2357–0052 has $[\text{Fe}/\text{H}] = -3.4$ and $[\text{Eu}/\text{Fe}] = +1.9$, and

²Department of Astronomical Science, The Graduate University of Advanced Studies, Mitaka, Tokyo, 181-8588 Japan

⁶INAF-Osservatorio Astronomico di Torino, Italy

exhibits a scaled solar r-process abundance pattern of heavy neutron-capture elements. This is the first example of an extremely metal-poor, main-sequence star showing large excesses of r-process elements; all previous examples of the large r-process-enhancement phenomena have been associated with metal-poor giants. The metallicity of this object is the lowest, and the excess of Eu ($[\text{Eu}/\text{Fe}]$) is the highest, among the r-process-enhanced stars found so far. We consider possible scenarios to account for the detection of such a star, and discuss techniques to enable searches for similar stars in the future.

Subject headings: nuclear reactions, nucleosynthesis, abundances — stars: abundances — stars: Population II

1. Introduction

Over the course of the past decade, a great deal of observational effort has been dedicated to studies of the chemical enrichment of the early universe through high-resolution spectroscopic measurements of the elemental abundances of metal-poor stars in the Galaxy. Of particular interest are the extremely metal-poor (EMP) stars, with $[\text{Fe}/\text{H}] \lesssim -3$ ¹, as such stars are expected to have recorded the nucleosynthesis products associated with the first generations of stars, perhaps even by individual supernovae, according to models such as the supernova-induced, low-mass star formation scenario (e.g. Audouze & Silk 1995; Shigeyama & Tsujimoto 1998).

A number of interesting abundance patterns have been noted to occur for individual EMP stars; the most remarkable example is perhaps the occurrence of the so-called r-process-enhanced stars (e.g. Sneden et al. 2003; Cayrel et al. 2001). Some EMP stars have been shown to exhibit over-abundances of the heavy neutron-capture elements, such as Eu with respect to Fe, by more than an order of magnitude, while the abundance patterns of their heavy elements agree well with that of a scaled solar r-process component (Sneden et al. 2008). Such stars may well represent the yields of an essentially pure r-process production event, the yields of which were apparently not fully mixed into the interstellar medium during early stages of the Galaxy’s evolution.

The astrophysical site(s) of the r-process is/are not yet established with confidence. However, an important clue may be the fact that all extremely r-process-enhanced stars (r-II stars; Beers & Christlieb 2005) identified to date have been found in a relatively narrow metallicity range ($-3 < [\text{Fe}/\text{H}] < -2.5$). The upper metallicity bound for the presence of r-II stars is well constrained by measurements for a large sample of stars in this metallicity range ($[\text{Fe}/\text{H}] \gtrsim -2.5$), and could be explained by the increase of the Fe abundance with a limited supply of Eu from individual supernovae².

¹ $[\text{A}/\text{B}] = \log(N_{\text{A}}/N_{\text{B}}) - \log(N_{\text{A}}/N_{\text{B}})_{\odot}$, and $\log \epsilon_{\text{A}} = \log(N_{\text{A}}/N_{\text{H}}) + 12$ for elements A and B.

²An exception is COS 82 in the dwarf spheroidal galaxy Ursa Minor, which exhibits $[\text{Fe}/\text{H}] = -1.5$ and $[\text{r}/\text{Fe}] = +1.5$

By contrast, high-resolution spectroscopic measurements for the lower metallicity range, $[\text{Fe}/\text{H}] < -3$, are still few in number. Thus, to obtain stronger constraints on the nature of the r-process, and in particular to possibly narrow the mass range of supernovae that may be capable of producing the r-process elements, further investigations for neutron-capture elements in EMP stars are strongly desired.

Here we report elemental abundance measurements for two EMP stars discovered during the course of the Sloan Digital Sky Survey (SDSS; York et al. 2000). These stars are the first known examples of cool main-sequence stars (subdwarfs) with $[\text{Fe}/\text{H}] < -3$, one of which exhibits extremely large excesses of the r-process elements.

2. Observations and Analysis

2.1. Sample Selection and Observations

The two cool subdwarfs investigated in the present work were selected from a large sample of candidate EMP stars observed during the Sloan Extension for Galactic Exploration and Understanding (SEGUE; Yanny et al. 2009), based on atmospheric parameters obtained by the SEGUE Stellar Parameter Pipeline (SSPP; Lee et al. 2008). These stars were listed as EMP stars with strong CH bands and $\log g \sim 3.5$, and were expected to be examples of carbon-enhanced metal-poor stars.

High-resolution follow-up spectroscopy was conducted with the Subaru Telescope High Dispersion Spectrograph (HDS; Noguchi et al. 2002) in 2008 August and October. The “snapshot” high-resolution ($R=30,000$), moderate S/N (~ 30) observations revealed these two stars to have high surface gravities, based on the weak absorption lines of ionized species (e.g., Fe II) and the broad wings of their Mg I b lines. The strong CH bands are explained by the high pressure in the subdwarf’s atmospheres, rather than due to a carbon excess. The metallicity of these two stars are significantly lower than previously known cool subdwarfs (e.g., Yong & Lambert 2003), except for the dwarf carbon star G77-61 (Plez & Cohen 2005). Moreover, very strong Ba II absorption lines were found for SDSS J2357–0052, suggesting large excesses of the heavy neutron-capture elements.

In order to determine detailed chemical compositions of these stars, we obtained higher resolution ($R = 60,000$), higher S/N spectra, covering 3500–6800 Å, with Subaru/HDS in 2008-2009. Table 1 lists details of the observations. The observed spectra around the Eu II 3819 Å feature are shown in Figure 1. For comparison purposes, we also obtained a spectrum with the same instrumental setup for the cool, very metal-poor ($[\text{Fe}/\text{H}] \sim -2$) subdwarf G 19–25, selected from Yong & Lambert (2003).

(Aoki et al. 2007). However, such an object has not yet been found among the Milky Way field stars.

2.2. Data Reduction and Measurements

Standard data reduction procedures were carried out with the IRAF echelle package³. The sky background was removed when the spectra are affected by the moon, as they were for several of the exposures.

Equivalent widths (W 's) for isolated absorption lines were measured by fitting Gaussian profiles as well as by direct integration of the absorption features. We found that the values obtained by direct integration are slightly higher for strong lines, probably due to inadequate fits of the assumed Gaussian profiles to the line wings. Hence, we adopted the values obtained by direct integration when the $\log(W/\lambda)$ value is larger than -4.7 , which corresponds to $W = 100 \text{ m}\text{\AA}$ at $\lambda = 5000 \text{ \AA}$, while the results of Gaussian fitting are adopted for weaker lines. We used the line list compiled by Aoki et al. (2010, in preparation) for studies of extremely metal-poor stars in the Galactic halo.

Radial velocities were measured for our program stars using selected Fe lines in the wavelength region 4050–5200 \AA . Heliocentric radial velocities are listed in Table 1 for individual spectra obtained in each run with the same setup. The radial velocities of SDSS J2357–0052 measured from the November 2008 and June/July 2009 spectra are about 1 km s^{-1} different from measurements obtained during August/October 2008. This difference is significantly larger than the random errors of the measurements (Table 1), which are estimated from $\sigma_v N^{-1/2}$, where σ_v is the standard deviation of the derived values for individual lines and N is the number of lines used. However, taking the systematic errors of the measurements into account, which could be as large as 0.5 km s^{-1} , further confirmations for the variation of radial velocity are required to derive any conclusion on the possible binarity of this object.

2.3. Atmospheric Parameters

The effective temperatures (T_{eff} 's) of our objects are determined from the $(V - K)_0$ colors and the temperature scale of Alonso, Arribas, & Martínez-Roger (1996b), assuming $[\text{Fe}/\text{H}] = -3.0$ for the SDSS objects. The V_0 magnitude is derived from the SDSS g_0 and $(g - r)_0$, using the transformations of Zhao & Newberg (2006). The K magnitude is adopted from the 2MASS catalogue (Skrutskie et al. 2006), using the reddening estimates by Schlegel et al. (1998). The photometry data and derived effective temperatures are given in Table 1 and 2, respectively. The derived T_{eff} 's of the two SDSS stars are quite similar. In the table, we also give the estimate of T_{eff} obtained from $(g - r)_0$ and a temperature scale constructed based on the ATLAS model atmospheres⁴. These T_{eff} 's are higher by 100–150 K than those from $(V - K)_0$ derived above. We adopt the averages of

³IRAF is distributed by the National Optical Astronomy Observatories, which is operated by the Association of Universities for Research in Astronomy, Inc. under cooperative agreement with the National Science Foundation.

⁴wwwuser.oat.ts.astro.it/castelli/colors/sloan.html

the two determinations. Application of the recent effective temperature scale of Casagrande et al. (2010) yields temperature estimates about 100 K higher T_{eff} than Alonso et al.’s scale for the same value of $(V - K)_0$; this result agrees well with the values adopted in the present work. The T_{eff} of G 19–25 is adopted from Alonso, Arribas, & Martínez-Roger (1996a) determined by the Infrared Flux Method, which was also adopted by Yong & Lambert (2003).

The surface gravity ($\log g$) for the SDSS stars is estimated from the isochrones of Kim et al. (2002) for metal-poor ($[\text{Fe}/\text{H}] = -3.5$) stars, adopting ages of 12 Gyr and assuming these stars are on the main sequence. The surface gravities ($\log g = 4.8$) are insensitive to the assumed metallicity and ages for such cool main-sequence stars. The $\log g$ of G 19–25 is estimated by demanding the Fe abundances derived from Fe I and Fe II agree. The metallicity adopted in the abundance analysis is $[\text{Fe}/\text{H}] = -3.3$ and -1.9 for the SDSS stars and G 19–25, respectively, which are obtained by iterations of the analysis procedure described below.

Elemental abundances are measured by standard analyses for equivalent widths using ATLAS model atmospheres with no convective overshooting (Castelli & Kurucz 2003), with enhancements of the α -elements. We performed analyses for more than 60 Fe I lines in the SDSS stars, whose equivalent widths range from 5 mÅ to 200 mÅ. Our analyses show that a decreasing trend of derived abundances with increasing equivalent widths emerges when the van der Waals broadening based on Unsöld (1955)’s treatment is enhanced, as was done in our previous studies (e.g. Aoki et al. 2002), even though no micro-turbulence is assumed. Hence, we adopt the Unsöld (1955)’s broadening with no modification in our analysis. We note that the iron abundance derived from weak lines ($\log(W/\lambda) < -5$), as well as the abundances for most of the neutron-capture elements (e.g., Y, La, Eu), also based on weak lines, are insensitive to the nature of the pressure broadening.

We confirmed that there remains no significant correlation between the derived Fe abundances from individual Fe I lines and their excitation potential, supporting the estimates of their effective temperatures from broadband colors.

The absolute magnitude of subdwarfs with $T_{\text{eff}} = 5000$ K is $M_V = 7.4$, according to the isochrones of Kim et al. (2002). This indicates that the stellar mass is $0.52 M_{\odot}$, and the distances of SDSS J2357–0052 ($V = 15.6$) and SDSS J1703+2836 ($V = 15.3$) are 440 pc and 370 pc, respectively. Adopting these distances as well as radial velocities and proper motions (SDSS J2357–0052: $\mu_{\alpha}, \mu_{\delta} = 46, -172$ mas yr $^{-1}$; SDSS J1703+2836: $\mu_{\alpha}, \mu_{\delta} = -27, -129$ mas yr $^{-1}$, with errors of ~ 2.5 mas yr $^{-1}$; Munn et al. 2004), the kinematics of the SDSS stars are calculated using the procedures of Chiba & Beers (2000). SDSS J2357–0052 is tentatively assigned to the outer-halo component (Carollo et al. 2007, 2010), based on its retrograde orbit ($V_{\phi} = -83 \pm 70$ km s $^{-1}$), its moderate eccentricity ($e = 0.47$), and its large Z_{max} value (the maximum distance of its orbit from the Galactic plane) of 8 kpc, coupled with its location in a Toomre energy diagram ($V = -306, (U^2 + W^2)^{1/2} = 191$ km s $^{-1}$); the kinematics of SDSS J1703+2836 are more consistent with the inner halo.

2.4. Abundance Measurements

The derived elemental abundances for our stars are listed in Table 2. Although only one Fe II line is clearly detected in the spectra of the SDSS stars, the derived iron abundance from the Fe II line agrees with that from Fe I lines within the measurement error. Moreover, the Ti abundances from the two ionization stages agree well in both objects. These results clearly exclude the possibility that these stars are cool giants with $\log g \sim 2$, but support the above estimates of the gravities.

The spectrum synthesis technique is adopted to determine the carbon abundance from the CH molecular band at 4315 Å. Although the derived abundance ratios are slightly higher than solar, these values are typical for unevolved, extremely metal-poor stars (e.g. Spite et al. 2005), thus these stars are not carbon-enhanced objects.

Barium abundances are obtained by an analysis including hyperfine splitting and isotope shifts (McWilliam 1998), assuming the isotope ratios expected for the r-process-enhanced case (see below). The final result is derived from the three weaker lines in the red region, which are less sensitive to hyperfine splitting. Hyperfine splitting is also included in the analysis of Mn I lines.

The abundances of Eu, Er, and Yb are determined by the spectrum synthesis technique, carefully checking on the effects of blending from other absorption features, for Eu II 3819, 4129 and 4205 Å, Er II 3692 Å, and Yb II 3694 Å. Atomic line data for Eu, Er, and Yb are adopted from Lawler et al. (2001), Lawler et al. (2008), and Sneden et al. (2009), respectively, including the effect of hyperfine splitting for Eu and Yb. The upper limit on the Th abundance is determined by the spectrum synthesis technique for the Th II 4019 Å line.

Random errors in the abundance measurements are estimated to be $\sigma N^{-1/2}$, where σ is the standard deviation of derived abundances from individual lines and N is the number of lines used in the analysis. When only a few lines are available, the σ of Fe I is adopted in the estimates. The errors due to the uncertainty of the atmospheric parameters ($\delta T_{\text{eff}} = 150$ K, $\delta \log g = 0.3$, $\delta v_{\text{micro}} = 0.2$ km s⁻¹) are also estimated, and added in quadrature to the random errors. The metallicity of G 19–25 obtained by our analysis agrees, within the errors, with that derived by Yong & Lambert (2003), adopting the same T_{eff} .

3. Discussion

The two SDSS stars studied in the present work turned out to be the lowest metallicity cool subdwarfs yet known, with $[\text{Fe}/\text{H}] < -3$. Metal-poor subdwarfs have been extensively studied by Yong & Lambert (2003), yet their most metal-poor objects have $[\text{Fe}/\text{H}] \sim -2.5$. The much larger, and deeper SDSS/SEGUE surveys are clearly potentially interesting sources for the discovery of additional examples of extremely metal-poor, cool subdwarfs.

These two stars exhibit quite similar abundance ratios of their lighter elements ($Z \leq 28$). The over-abundances of the α -elements and under-abundances of Mn are similar to those found for other EMP stars. Other iron-peak elements trace the Fe abundances, while EMP giants usually show under-abundances of Cr as well as over-abundances of Co. However, discrepancies of Cr abundance ratios between EMP giants and main-sequence turn-off stars are known to occur (e.g. Lai et al. 2008), and our results are similar to those of turn-off stars. Lithium is not detected for either star, and the upper limits on its abundance are significantly lower than the Spite plateau value, as expected for cool stars with substantial convective envelopes.

A surprising result is that one of the first two subdwarfs with $[\text{Fe}/\text{H}] < -3$ studied by high-resolution spectroscopy exhibits large excesses of neutron-capture elements. Figure 2 shows the abundances ($\log \epsilon$ values) of neutron-capture elements in SDSS J2357–0052. Comparisons with the abundance patterns of the r- and s-process components in solar-system material indicate that the origin of neutron-capture elements is clearly associated with the r-process. This result immediately confirms that large excesses of r-process elements are not a phenomena found only for red giants (see Sneden et al. 2008).

The $[\text{Eu}/\text{Fe}]$ abundance ratio of SDSS J2357–0052 ($[\text{Eu}/\text{Fe}] = +1.9$) is the highest among the stars that exhibit excesses of r-process elements at low metallicity (Fig. 3). This is basically because of the low Fe abundance of this object ($[\text{Fe}/\text{H}] = -3.4$). Indeed, the Eu abundance of this object ($[\text{Eu}/\text{H}] = -1.4$) is similar to those previously found for other r-II stars, e.g., CS 31082-001: $[\text{Eu}/\text{H}] = -1.28$ (Hill et al. 2002); HE 1523–0901 : $[\text{Eu}/\text{H}] = -1.14$ (Frebel et al. 2007).

The large excesses of heavy neutron-capture elements in r-II stars are usually interpreted as a result of the pollution of interstellar matter by a supernova (or some other event) that yields amounts of r-process elements and subsequent low-mass star formation from the enriched material. The fact that only a small fraction of stars show such excesses (roughly 5% of stars with $[\text{Fe}/\text{H}] < -2$ according to Barklem et al. 2005) indicates that the event(s) associated with the production of r-process elements were rare, and did not produce significant amounts of Fe.

Since r-II stars have previously only been found in the metallicity range $[\text{Fe}/\text{H}] \gtrsim -3$ (Fig. 3), the respective sites of the r-process have been supposed to be supernovae of less massive progenitors (e.g. 8–10 M_{\odot} ; Wanajo & Ishimaru 2006). Our discovery of SDSS J2357–0052 indicates that the metallicity range in which highly r-process-enhanced stars appear extends to as low as $[\text{Fe}/\text{H}] = -3.4$, and thus opens the possibility that a larger range of progenitor masses may have been involved.

The apparent upper bound of $[\text{Eu}/\text{H}]$ in r-II stars might indicate the existence of a limit of the enrichment by a supernova yielding r-process elements. The mass ratio of Eu/H corresponding to $[\text{Eu}/\text{H}] \sim -1.5$ is $M_{\text{Eu}}/M_{\text{H}} \sim 10^{-11}$. If the Eu mass produced by a single supernova is assumed to be $10^{-7}M_{\odot}$ (Wanajo & Ishimaru 2006), the amount of interstellar matter polluted by that could only be on the order of 10^4M_{\odot} . The Fe production by such stars is estimated to be $\sim 2 \times 10^{-3}M_{\odot}$ (Wanajo et al. 2009). If this is mixed into a metal-free cloud of 10^4M_{\odot} , the resulting metallicity

is $[\text{Fe}/\text{H}] \sim -4$. If the cloud mass is assumed to be smaller, taking account of the low explosion energy of a supernova by a less massive progenitor, the Fe abundance of SDSS J2357–0052, as well as those of neutron-capture elements, could be explained by the contribution of a single supernova.

Another scenario to explain the large excesses of r-process elements in SDSS J2357–0052 is that the object belongs to a binary system in which the massive companion has exploded, yielding the r-process elements. A possible binary system with a highly elliptical orbit is suggested for the r-process-enhanced star HE 2327–5642 ($[\text{Fe}/\text{H}] = -2.78$; $[\text{Eu}/\text{Fe}] = +0.98$) by Mashonkina et al. (2010), based on a single radial velocity measurement showing significant departure ($\sim 20 \text{ km s}^{-1}$) from 16 others (with errors on the order of 0.2–0.5 km s^{-1}). Since this observation (if not spurious) may have some relationship with the phenomena of large r-process excess, further investigations of radial velocity changes for r-II stars (including SDSS J2357–0052) are strongly desired.

It may be of interest that the first extremely metal-poor r-II subdwarf appears to be associated with the outer halo. Given the possible distinct astrophysical origins between the inner- and outer-halo populations (e.g., masses of their progenitor sub-haloes, and/or star formation histories; Carollo et al. 2007, 2010), it would clearly be desirable to establish membership assignments for the known r-II stars. This can be realized with sufficient accuracy if additional r-II subdwarfs are found. This could be accomplished by targeting candidate very and extremely metal-poor stars identified by SDSS/SEGUE with high proper motions (likely subdwarfs) and low T_{eff} .

Facilities: SDSS, Subaru(HDS).

Funding for the SDSS and SDSS-II has been provided by the Alfred P. Sloan Foundation, the Participating Institutions, the National Science Foundation, the U.S. Department of Energy, the National Aeronautics and Space Administration, the Japanese Monbukagakusho, the Max Planck Society, and the Higher Education Funding Council for England. The SDSS Web Site is <http://www.sdss.org/>.

The SDSS is managed by the Astrophysical Research Consortium for the Participating Institutions. The Participating Institutions are the American Museum of Natural History, Astrophysical Institute Potsdam, University of Basel, University of Cambridge, Case Western Reserve University, University of Chicago, Drexel University, Fermilab, the Institute for Advanced Study, the Japan Participation Group, Johns Hopkins University, the Joint Institute for Nuclear Astrophysics, the Kavli Institute for Particle Astrophysics and Cosmology, the Korean Scientist Group, the Chinese Academy of Sciences (LAMOST), Los Alamos National Laboratory, the Max-Planck-Institute for Astronomy (MPIA), the Max-Planck-Institute for Astrophysics (MPA), New Mexico State University, Ohio State University, University of Pittsburgh, University of Portsmouth, Princeton University, the United States Naval Observatory, and the University of Washington.

W. A. would like to acknowledge useful discussions on the r-process with S. Wanajo and Y. Ishimaru. W. A. is supported by a Grant-in-Aid for Science Research from JSPS (grant 18104003).

T.C.B. acknowledges partial funding of this work from grants PHY 02-16783 and PHY 08-22648: Physics Frontier Center/Joint Institute for Nuclear Astrophysics (JINA), awarded by the U.S. National Science Foundation. D.C. acknowledges funding from RSAA ANU to pursue her research.

REFERENCES

- Alonso, A., Arribas, S., & Martínez-Roger, C. 1996a, *A&AS*, 117, 227
- Alonso, A., Arribas, S., & Martínez-Roger, C. 1996b, *A&A*, 313, 873
- Aoki, W., et al. 2005, *ApJ*, 632, 611
- Aoki, W., Honda, S., Sadakane, K., & Arimoto, N. 2007, *PASJ*, 59, L15
- Aoki, W., Norris, J. E., Ryan, S. G., Beers, T. C., & Ando, H. 2002, *ApJ*, 567, 1166
- Arlandini, C., Käppeler, F., Wisshak, K., Gallino, R., Lugaro, M., Busso, M., & Straniero, O. 1999, *ApJ*, 525, 886
- Audouze, J., & Silk, J. 1995, *ApJ*, 451, L49
- Barklem, P. S., et al. 2005, *A&A*, 439, 129
- Beers, T. C., & Christlieb, N. 2005, *ARAA*, 43, 531
- Carollo, D., et al. 2007, *Nature*, 450, 1020
- Carollo, D., et al. 2010, *ApJ*, 712, 692
- Casagrande, L., Ramírez, I., Meléndez, J., Bessell, M., & Asplund, M. 2010, *A&A*, 512, A54
- Castelli, F., & Kurucz, R. L. 2003, *Modelling of Stellar Atmospheres*, 210, 20P
- Cayrel, R., et al. 2001, *Nature*, 409, 691
- Chiba, M., & Beers, T. C. 2000, *AJ*, 119, 2843
- Christlieb, N., et al. 2004, *A&A*, 428, 1027
- François, P., et al. 2007, *A&A*, 476, 935
- Frebel, A., Christlieb, N., Norris, J. E., Thom, C., Beers, T. C., & Rhee, J. 2007, *ApJ*, 660, L117
- Hill, V., et al. 2002, *A&A*, 387, 560
- Honda, S., Aoki, W., Kajino, T., Ando, H., Beers, T. C., Izumiura, H., Sadakane, K., & Takada-Hidai, M. 2004, *ApJ*, 607, 474

- Hayek, W., et al. 2009, *A&A*, 504, 511
- Ishimaru, Y., Wanajo, S., Aoki, W., & Ryan, S. G. 2004, *ApJ*, 600, L47
- Kim, Y.-C., Demarque, P., Yi, S. K., & Alexander, D. R. 2002, *ApJS*, 143, 499
- Lai, D. K., Bolte, M., Johnson, J. A., Lucatello, S., Heger, A., & Woosley, S. E. 2008, *ApJ*, 681, 1524
- Lawler, J. E., Wickliffe, M. E., den Hartog, E. A., & Sneden, C. 2001, *ApJ*, 563, 1075
- Lawler, J. E., Sneden, C., Cowan, J. J., Wyart, J.-F., Ivans, I. I., Sobeck, J. S., Stockett, M. H., & Den Hartog, E. A. 2008, *ApJS*, 178, 71
- Lee, Y. S., et al. 2008, *AJ*, 136, 2022
- Mashonkina, L., Christlieb, N., Barklem, P. S., Hill, V., Beers, T. C., & Velichko, A. 2010, *A&A*, 516, A46
- McWilliam, A. 1998, *AJ*, 115, 1640
- Munn, J. A., et al. 2004, *AJ*, 127, 3034
- Noguchi, K. et al. 2002, *PASJ*, 54, 855
- Plez, B., & Cohen, J. G. 2005, *A&A*, 434, 1117
- Preston, G. W., Sneden, C., Thompson, I. B., Shectman, S. A., & Burley, G. S. 2006, *AJ*, 132, 85
- Roederer, I. U., Sneden, C., Thompson, I. B., Preston, G. W., & Shectman, S. A. 2010, *ApJ*, 711, 573
- Schlegel, D., Finkbeiner, D., & Davis, M. 1998, *ApJ*, 500, 525
- Shigeyama, T., & Tsujimoto, T. 1998, *ApJ*, 507, L135
- Skrutskie, M. F., et al. 2006, *AJ*, 131, 1163
- Sneden, C., Cowan, J. J., & Gallino, R. 2008, *ARA&A*, 46, 241
- Sneden, C., et al. 2003, *ApJ*, 591, 936
- Sneden, C., Lawler, J. E., Cowan, J. J., Ivans, I. I., & Den Hartog, E. A. 2009, *ApJS*, 182, 80
- Spite, M., et al. 2005, *A&A*, 430, 655
- Suda, T., et al. 2008, *PASJ*, 60, 1159
- Unsöld, A., 1955, *Physik der Sternatmosphären* (2nd ed., Berlin: Springer)

Wanajo, S., & Ishimaru, Y. 2006, Nuclear Physics A, 777, 676

Wanajo, S., Nomoto, K., Janka, H.-T., Kitaura, F. S., Müller, B. 2009, ApJ, 695, 208

Yanny, B., et al. 2009, AJ, 137, 4377

Yong, D., & Lambert, D. L. 2003, PASP, 115, 796

York, D. G., et al. 2000, AJ, 120, 1579

Zhao, C., & Newberg, H. J. 2006, arXiv:astro-ph/0612034

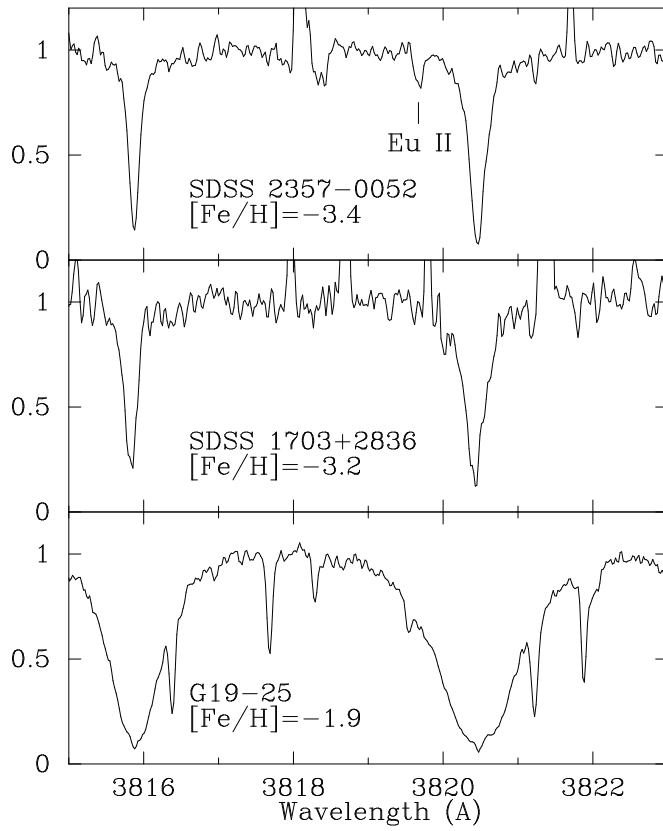


Fig. 1.— Observed spectra around the Eu II 3819 Å line. The stellar name and derived $[Fe/H]$ are given in each panel.

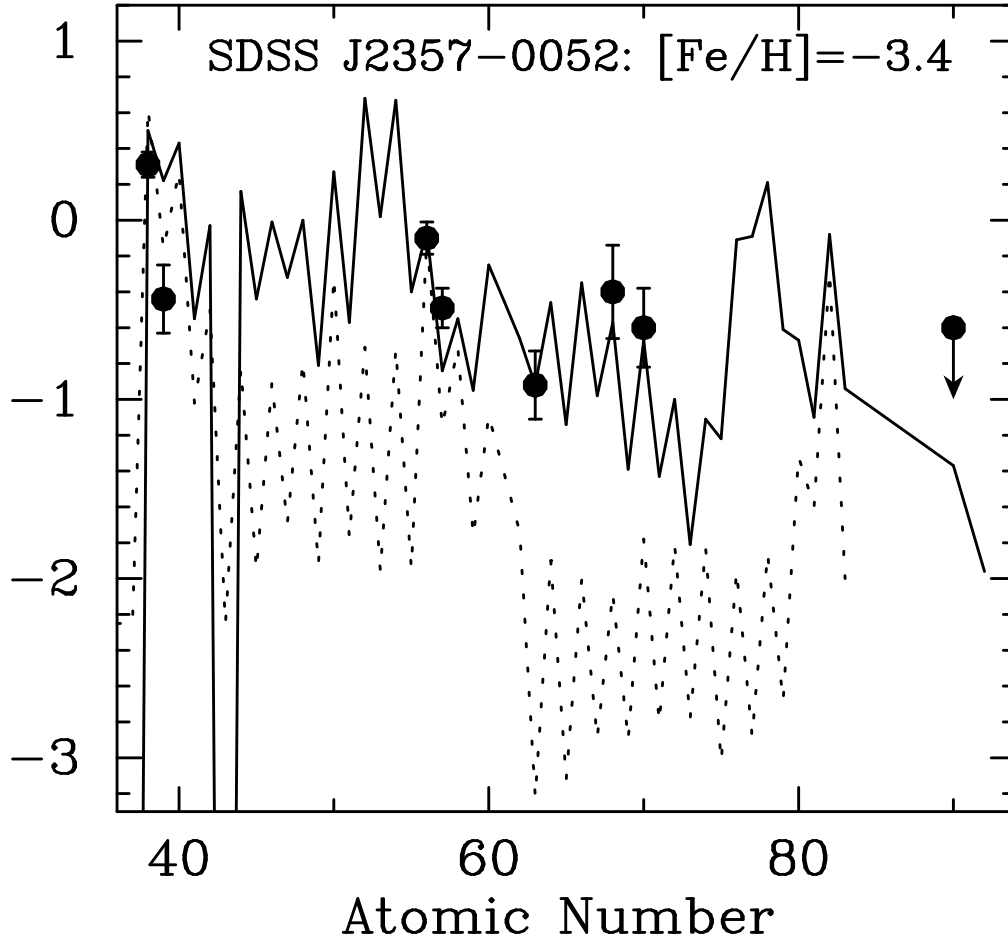


Fig. 2.— The abundances ($\log \epsilon$ values) of neutron-capture elements in SDSS J2357-0052 (dots). The solid and dotted lines indicate the abundance patterns of the r- and s-process components in Solar System material (Arlandini et al. 1999), normalized at Ba ($Z = 56$).

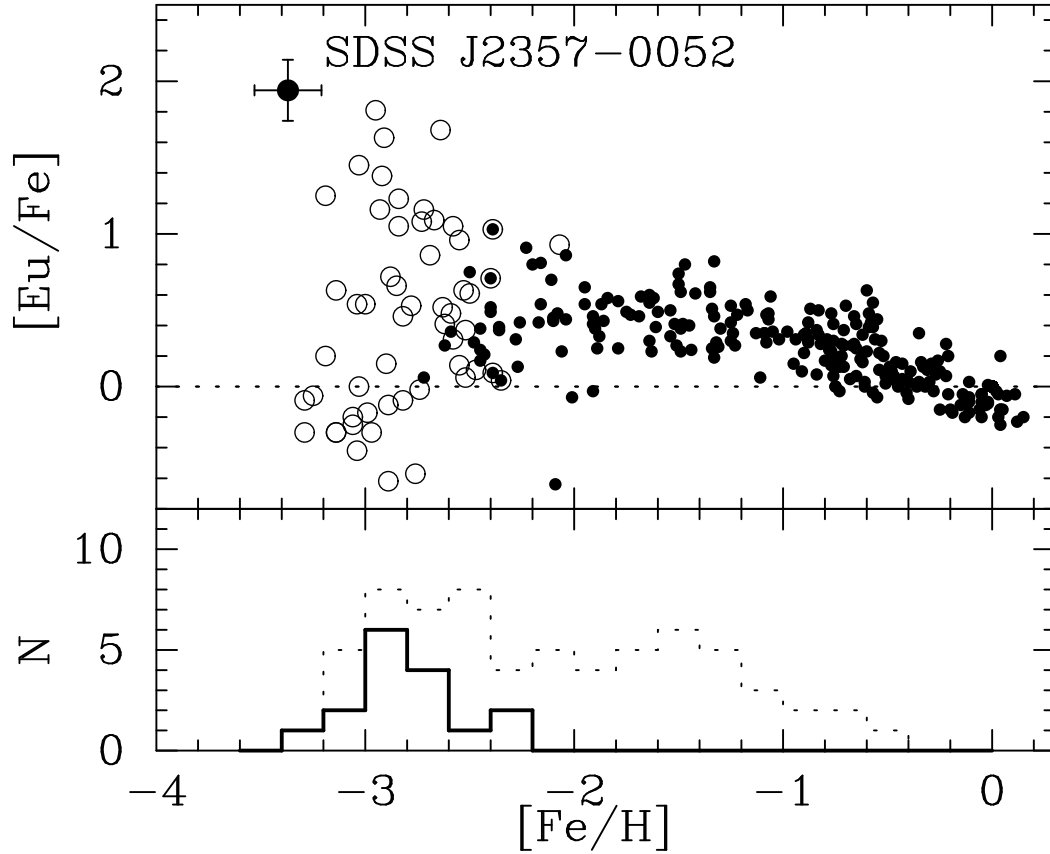


Fig. 3.— The Eu abundance ratios of Galactic halo and disk stars (upper panel). The large filled circle indicates our result for SDSS J2357–0052, while open circles are for very metal-poor stars taken from literature (Hill et al. 2002; Sneden et al. 2003; Honda et al. 2004; Ishimaru et al. 2004; Christlieb et al. 2004; Aoki et al. 2005; Barklem et al. 2005; Preston et al. 2006; François et al. 2007; Frebel et al. 2007; Hayek et al. 2009; Roederer et al. 2010). Results for less metal-poor stars shown by the small filled circles are taken from the SAGA database (Suda et al. 2008). The lower panel shows the distribution of r-II stars ($[Eu/Fe] > +1.0$, solid line) and r-II + r-I ($[Eu/Fe] > +0.5$) stars (dotted line), following the nomenclature of Beers & Christlieb (2005).

Table 1. OBJECTS AND OBSERVING LOG

Star ^a	Obs. date (UT)	Setup ^b	Exposure (min.)	Count (5000 Å)	HJD	V_{helio} (km s^{-1})
SDSS J2357–0052	Aug 21, 2008	Yd	15	430	2454700	-9.1 ± 0.3
$V_0 = 15.612$	Oct 4, 2008	Yd	15	480	2454744	-9.3 ± 0.1
$(V - K)_0 = 2.059$	Nov. 16, 2008	Bc	160	2890	2454786	-10.0 ± 0.1
$(g - r)_0 = 0.612$	June 30/July 2, 2009	Bc	180	2610	2455012/14	-10.2 ± 0.1
$E(B - V) = 0.030$	Sep 11, 2009	Yd	80	1620	2455086	-9.0 ± 0.1
	Sep 12, 2009	Bc	120	1690	2455087	-9.2 ± 0.1
SDSS J1703+2836	July 6, 2008	Yd	10	390	2454654	-178.2 ± 0.2
$V_0 = 15.342$	July 2, 2009	Bc	120	1650	2455015	-178.0 ± 0.1
$(V - K)_0 = 2.098$	Sep 11, 2009	Yd	120	1080	2455086	-178.1 ± 0.1
$(g - r)_0 = 0.593$	Sep 12, 2009	Bc	120	1970	2455087	-177.7 ± 0.1
$E(B - V) = 0.065$
G 19–25	Sep 10, 2009	Yd	10	7700	2455086	-32.4 ± 0.2
$V_0 = 11.64$	Sep 11, 2009	Bc	10	8000	2455087	-32.5 ± 0.1
$(V - K)_0 = 2.023$
$E(B - V) = 0.000$

^aThe full names are SDSS J235718.91–005247.8 and SDSS J170339.60+283649.9. The PLATE-MJD-FIBER names in the SDSS/SEGUE databases are 1489-52991-251 and 2808-54524-510, respectively.

^bThe HDS standard setups Yd and Bc cover 4100–6800 Å and 3550–5250 Å, respectively

